Unusual catalyst-free epitaxial growth of silicon nanowires by thermal evaporation

Y. Qin, X. N. Zhang, K. Zheng, H. Li, X. D. Han, and Z. Zhang

Citation: Applied Physics Letters **93**, 063104 (2008); doi: 10.1063/1.2967875
View online: http://dx.doi.org/10.1063/1.2967875
View Table of Contents: http://scitation.aip.org/content/aip/journal/apl/93/6?ver=pdfcov
Published by the AIP Publishing

Unusual catalyst-free epitaxial growth of silicon nanowires by thermal evaporation

Y. Qin, X. N. Zhang,[a] K. Zheng, H. Li, X. D. Han,[a] and Z. Zhang
Institute of Microstructure and Property of Advanced Materials, Beijing University of Technology, Beijing 100124, People's Republic of China

(Received 19 June 2008; accepted 7 July 2008; published online 14 August 2008)

We report a catalyst-free epitaxial growth of silicon nanowires on polyhedral facets of mother Si nanoparticles by thermal evaporation process. Single silicon nanowires and octopuslike silicon nanowires (OSNWs) were synthesized under different temperatures. The OSNWs have several directions including ⟨112⟩, ⟨110⟩, and the unusual directions of ⟨100⟩ and ⟨111⟩. A catalyst-free temperature-dependent epitaxial growth model was suggested. Using the Wulff theory and first principle calculations, these growth directions can be explained by the preferential selection of temperature-dependent surface energies. It thus revealed an important but simple growth model in which the growth directions could be delicately controlled through only determining temperature and substrate orientation. © *2008 American Institute of Physics*. [DOI: 10.1063/1.2967875]

Silicon nanowires (Si NWs) have attracted much attention in the past ten years[1,2] for their outstanding physical properties and the central role of Si integrated circuit technology. Remarkable progress has been reported for the synthesis of the Si NWs (Refs. 3–5) and applications to electron devices[6–9] such as diodes, logic gates, single electron transistors, and sensors. The different crystallographic oriented Si NWs exhibited distinct properties due to the crystal structure anisotropy.[10] Thus, it is important to control the growth direction for the various applications to the nanodevices.

There are two typical growth mechanisms for Si NWs. The first one is vapor-liquid-solid (VLS) mechanism,[11] and the second is oxide assistant growth (OAG) mechanism.[4] By VLS method, the growth direction of Si NWs was influenced by the diameter.[12–15] The growth direction is ⟨110⟩ for the diameter less than 10 nm, while the growth direction is ⟨111⟩ for the diameter larger than 20 nm. In the OAG process, the longitude directions are mainly ⟨112⟩ and ⟨110⟩, there were scarcely ⟨100⟩ and ⟨111⟩ (Ref. 16) oriented Si NWs.

In this work, two morphologies of Si NWs were synthesized by thermal evaporation. One is the freestanding single Si nanowires (SSNWs) with highly preferential growth direction of ⟨110⟩ while another is the octopuslike Si nanowires (OSNWs). Surprisingly, the OSNWs can possess unusual ⟨100⟩ and ⟨111⟩ growth directions, which have been very rare for Si NWs synthesized by thermal evaporation. The surface energy of typical low index faces was calculated under different temperatures. The change in the growth direction can be explained by the change in the relative surface energy according to the Wulff theory. A catalyst-free epitaxial growth mechanism was suggested to interpret this unusual growth of Si NWs.

SiO powder of 0.3 g as thermal evaporation source material was placed in the growth chamber firstly, and then the chamber was closed. Si wafer was used as substrate. After evacuation of the chamber to a pressure of 10^{-2} Pa, Ar gas was introduced into the reaction chamber until the pressure reached 5.4×10^{3} Pa. The SiO powder was heated to and maintained at the temperature of 1260 °C for 10 min. After growth, the silicon substrate surface coated with spongelike product showed different colors, changing from light yellow to yellow mixed with pink with temperature increasing. Microstructure characterization was carried out by field-emission scanning electron microscopy (SEM) (JEOL 6500F), transmission electron microscopy (TEM) (JEOL-2010), and field-emission TEM (JEOL-2010F).

The surface energy of different crystallographic planes was calculated by CASTEP and Discovery module in the MATERIAL STUDIO® program. The ⟨100⟩, ⟨110⟩, and ⟨111⟩ slice models were built up with about 1.5 nm atom layer and 1.0 nm vacuum layer. To relax these three models and the bulk silicon crystal, the molecular dynamics (MD) calculation with NPT (dynamics with a thermostat to maintain a constant temperature and a barostat to maintain a constant pressure) ensemble was performed. During the MD calculation, the pressure condition was set to 0 GPa, the temperatures were set 273, 873, 1173, and 1573 K, respectively, and the force filed was produced by COMPASS module automatically. The relax time was set to 200 ps with 200 000 steps to achieve the system balance that the fluctuation of the energy and the temperature is less than 5%–10%.

The morphology of the as synthesized products was strongly influenced by the temperature. Large quantities of SSNWs were observed at low temperature about 900 °C, as shown in Fig. 1(a). This kind of NWs is long, straight, and freestanding. Length of the SSNWs is about tens of microns and the diameter distributes from 30 to 60 nm. At the high temperature region around 1200 °C, the OSNWs were formed. One or more branches share one particle [Fig. 1(b)]. Figure 1(c) provides low magnified TEM image of a SSWN with core-shell structure. The core is about 40 nm in diameter and the shell is 10 nm in thickness. Selected area electron diffraction pattern (SAEDP) and high resolution TEM (HRTEM) results show that the core is crystal Si and the shell is amorphous SiO_2 [Figs. 1(d) and 1(e)]. Around 40 SSNWs were characterized, all of them have ⟨110⟩ growth directions and no other directions were found. Figures 1(f)–1(i) are the typical images of OSNWs, which show one

[a]Authors to whom correspondence should be addressed. Electronic addresses: xnzhang@bjut.edu.cn. Tel.: 86-10-67392281 and xdhan@bjut.edu.cn. Tel.: 86-10-67396087.

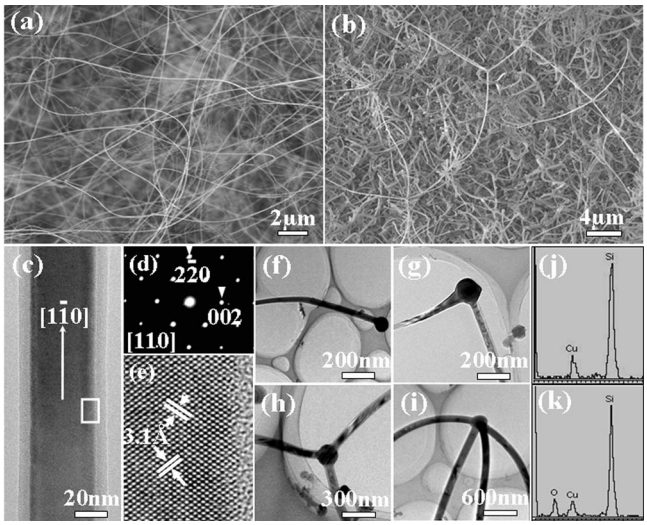

FIG. 1. The morphology and structure of the freestanding single NWs and the octopuslike NWs. (a) SEM image of the SSNWs; (b) SEM image of the OSNWs; (c) one SSNW along the ⟨110⟩ direction; (d) the SAED image of the SSNW; (e) HRTEM image of the white framed region indicated in (c); (f)-(i) TEM image of the OSNWs with different numbers of arms; (j) EDS result taken from the tip of the OSNWs; (k) EDS result taken from the NW of the OSNWs. The Cu signal was from the Cu supporting grid.

"arm," two arms, three arms, and four arms, respectively. The energy dispersive spectroscopy (EDS) results respectively taken from the tips and NWs revealed that the tips are mainly consisted of Si [Fig. 1(j)] and the NWs consisted of Si and O [Fig. 1(k)], in which oxygen element came from the outer shell of SiO_2.

The growth directions of the OSNWs were analyzed by HRTEM. Four kinds of growth directions including ⟨100⟩, ⟨110⟩, ⟨112⟩, and ⟨111⟩ were found, as shown in Figures 2(a)–2(d). We characterized the growth directions of arms and showed the statistical data in Fig. 2(e).

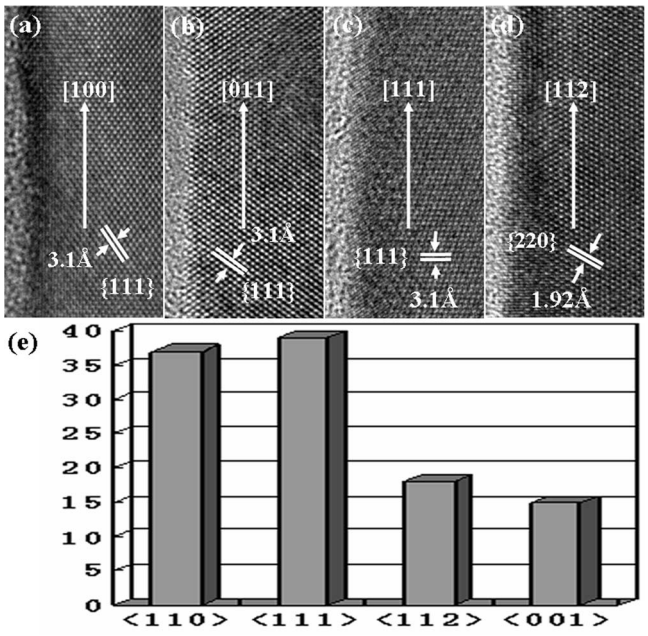

FIG. 2. The different growth directions of the octopuslike NWs. (a)–(d) are the HRTEM images of the OSNWs with different directions showing the high quality single crystalline features of the SiNW arms. The NWs growth directions are indicated by white arrows. (e) is the statistics of the growth directions of the arms of the OSNWs.

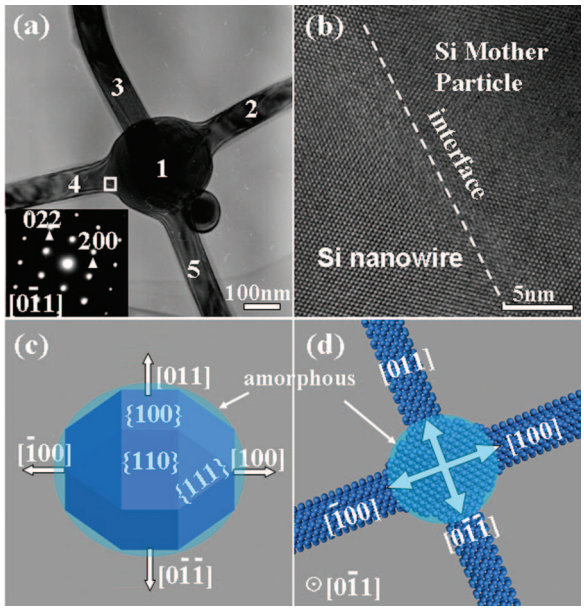

FIG. 3. (Color) The study of the epitaxial growth. (a) The TEM image and SAED pattern of the octopuslike nanostructure with four arms. (b) The HRTEM image of the interface of the Si mother particle and the Si NW. (c) The model of Si particle, (d) derived from (a), a model of OSNWs.

Figure 3(a) is the low magnified TEM image of the OSNW with four arms. The SAEDPs obtained from five regions indicated in Fig. 3(a) are completely same, which were inserted in Fig. 3(a). It is known that the particle and the NWs are single crystalline Si. The growth directions of NWs 2 and 4 were ⟨100⟩, and 3 and 5 were ⟨110⟩. From the HRTEM images [Fig. 3(b)], it can be clearly revealed that Si NWs grow epitaxially from the {110} and {100} facets of Si mother particle. From the microstructure analysis of the OSNWs, it can be deduced that the growth process can be divided into two steps. The first step is the growth of the "big head," and the second step is the growth of the arms. The big head acts as the substrate for a subsequent NW's epitaxial growth. By preferred exposing low energy facets, the shape of the big head was suggested to be a polyhedron with the low miller indices facets by {111}, {110}, and {100}. As shown in Fig. 3(c), the polyhedron has twelve {110} facets, eight {111} facets, and six exposed {100} surfaces. A corresponding atomic model of OSNW with four arms is proposed and shown in Fig. 3(d). The blue circles surrounding the particles represent the oxide in Figs. 3(c) and 3(d).

The above results revealed a temperature-dependent epitaxial growth phenomenon of Si NWs. This can be understood from the change of the surface energy as a function of temperature. First, we calculated the surface energy of three typical low miller index faces by MD method. Second, the change in the growth directions of the Si NWs as a function of temperature was explained using a simple model.

According to the Wulff law,[17] the surface with higher surface energy has the higher growth velocity. Therefore, the facets with low surface energy enclose the crystal in order to keep the total surface energy low. The total surface energy tends to be minimized. The surface energy decreases with temperature increasing.[18] The surface energies of {110}, {100}, and {111} faced under different temperatures by MD method were calculated from 273 to 1573 K. The surface energy can be defined as

TABLE I. The surface energies of {100}, {110}, and {111} at different temperatures.

	273 K	873 K	1273 K	1573 K
$\alpha_{\{100\}}$	0.129 86	0.127 25	0.125 34	0.124 66
$\alpha_{\{110\}}$	0.128 53	0.122 83	0.114 63	0.099 46
$\alpha_{\{111\}}$	0.118 03	0.114 29	0.110 94	0.103 74

$$\gamma_{\text{surface}}^{hkl} = \frac{(\gamma_{\text{tot}}^{\text{bulk}} - \gamma_{\text{tot}}^{hkl})}{(2 \times S_{hkl})},$$

where $\gamma_{\text{surface}}^{hkl}$ is the surface energy of the (hkl) plane, $\gamma_{\text{tot}}^{\text{bulk}}$ is the total energy of the bulk, $\gamma_{\text{tot}}^{hkl}$ is the total energy of the divided bulk along the (hkl) plane, and S_{hkl} is the area of the (hkl) plane.

After MD calculation, the energy of the relaxed structures of three slice models and the bulk model under the different temperature were calculated with CASTEP package. The calculation was conducted using ultrasoft pseudopotential, and E_{cutoff} was set to be 150 eV. The k point was selected automatically. The calculation results (Table I) show that the {100}, {110}, and {111} surface energies of silicon decreased with increasing temperature. Under 273 K, the relative surface energy is $\alpha_{\{100\}} > \alpha_{\{110\}} > \alpha_{\{111\}}$. These results are consistent to the experimental results by others.[19] While under 1573 K, the relative surface energy is changed as $\alpha_{\{100\}} > \alpha_{\{111\}} > \alpha_{\{110\}}$.

Having the surface energies under different temperatures, the total surface energies can be estimated. Based on the Si NWs' orientations, the total surface energies of the NWs with ⟨110⟩, ⟨111⟩, and ⟨100⟩ growth directions can be calculated (supporting materials). The change in total surface energies of the three kinds of NWs with temperature increasing was shown in Fig. 4. Under low temperature, the total surface energy of the NWs with ⟨110⟩ growth direction is lower than the NWs with ⟨111⟩ and ⟨100⟩ growth directions. This agrees with the experimental results that the growth direction is ⟨110⟩ under low temperature. While with increasing temperature, the total surface energy decreases. There is a crossing point around 1120 K between ⟨110⟩'s and ⟨100⟩'s. The total surface energy of the NWs with ⟨110⟩ growth direction becomes higher and the unusual ⟨111⟩ and ⟨100⟩ growth directions were observed above this crossing temperature. This is in good agreement with the experimental observations in this study.

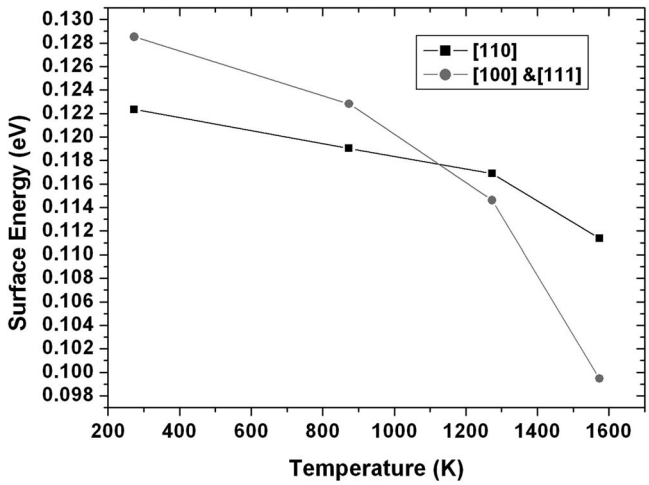

FIG. 4. The total surface energies of {110} and {111} facets as a function of temperature calculated by MD.

In summary, the unusual ⟨111⟩ and ⟨100⟩ directions of the OSNWs as well as the SSNWs with high preferential ⟨110⟩ growth direction were obtained without the help of catalysts. We provide a Si NW diameter independent growth model by which the accurate Si NWs with all diameters and desired crystallographic orientations could be expected by careful control of the epitaxial process with selecting a correct mother nanosubstrate and temperature.

This work was supported by National Basic Research Program of China-2007CB935400, National 973 program, National Science Foundation of China under Grant No. 50272081. X. D. Han also thanks the programs of NCET (05009015200701) and the Key Project of Beijing Education Committee (JB102001200801).

[1] Z. L. Wang, Adv. Mater. (Weinheim, Ger.) **12**, 1295 (2000).
[2] R. Agarwal and C. M. Liber, Appl. Phys. A: Mater. Sci. Process. **85**, 209 (2006).
[3] A. M. Morales and C. M. Lieber, Science **279**, 208 (1998).
[4] R. Q. Zhang, Y. Lifshitz, and S. T. Lee, Adv. Mater. (Weinheim, Ger.) **15**, 635 (2003).
[5] D. D. D. Ma, C. S. Lee, F. C. K. Au, S. Y. Tong, and S. T. Lee, Science **299**, 1874 (2003).
[6] Y. Cui and C. M. Lieber, Science **291**, 851 (2001).
[7] Y. Huang, X. F. Duan, Y. Cui, L. J. Lauhon, K. H. Kim, and C. M. Lieber, Science **294**, 1313 (2001).
[8] J. He, Z. A. K. Durrani, and H. Ahmed, Microelectron. Eng. **73**, 712 (2004).
[9] Y. Cui, Q. Q. Wei, H. K. Park, and C. M. Lieber, Science **293**, 1289 (2001).
[10] J. D. Holmes, K. P. Johnston, R. C. Doty, and B. A. Korgel, Science **287**, 1471 (2000).
[11] R. S. Wagner and W. C. Ellis, Appl. Phys. Lett. **4**, 89 (1964).
[12] Y. Wu, Y. Cui, L. Huynh, J. Barrelet, D. C. Bell, and C. M. Lieber, Nano Lett. **4**, 433 (2004).
[13] S. P. Ge, K. L. Jiang, X. X. Lu, Y. F. Chen, R. M. Wang, and S. S. Fan, Adv. Mater. (Weinheim, Ger.) **17**, 56 (2005).
[14] V. Schmidt, S. Senz, and U. Gösele, Nano Lett. **5**, 931 (2005).
[15] Y. Cui, L. J. Lauhon, M. S. Gudiksen, J. F. Wang, and C. M. Lieber, Appl. Phys. Lett. **78**, 2214 (2001).
[16] C. P. Li, C. S. Lee, X. L. Ma, N. Wang, R. Q. Zhang, and S. T. Lee, Adv. Mater. (Weinheim, Ger.) **15**, 607 (2003).
[17] K. C. Zhang and L. H. Zhang, *Crystal Growth* (Science, Beijing, 1981), pp. 77–85.
[18] R. L. Zheng and Y. Tao, Acta Phys. Sin. **55**, 1942 (2006).
[19] G. A. Wolff, J. Electrochem. Soc. **110**, 1293 (1963).